PHYSICAL REVIEW D, VOLUME 59, 052003

Υ dipion transitions at energies near the $\Upsilon(4S)$

S. Glenn, Y. Kwon,* A. L. Lyon, S. Roberts, and E. H. Thorndike
University of Rochester, Rochester, New York 14627

C. P. Jessop, K. Lingel, H. Marsiske, M. L. Perl, V. Savinov, D. Ugolini, and X. Zhou
Stanford Linear Accelerator Center, Stanford University, Stanford, California 94309

T. E. Coan, V. Fadeyev, I. Korolkov, Y. Maravin, I. Narsky, R. Stroynowski, J. Ye, and T. Wlodek
Southern Methodist University, Dallas, Texas 75275

M. Artuso, E. Dambasuren, S. Kopp, G. C. Moneti, R. Mountain, S. Schuh, T. Skwarnicki, S. Stone, A. Titov, G. Viehhauser, and J. C. Wang
Syracuse University, Syracuse, New York 13244

J. Bartelt, S. E. Csorna, K. W. McLean, S. Marka, and Z. Xu
Vanderbilt University, Nashville, Tennessee 37235

R. Godang, K. Kinoshita, I. C. Lai, P. Pomianowski, and S. Schrenk
Virginia Polytechnic Institute and State University, Blacksburg, Virginia 24061

G. Bonvicini, D. Cinabro, R. Greene, L. P. Perera, and G. J. Zhou
Wayne State University, Detroit, Michigan 48202

S. Chan, G. Eigen, E. Lipeles, J. S. Miller, M. Schmidtler, A. Shapiro, W. M. Sun, J. Urheim, A. J. Weinstein, and F. Würthwein
California Institute of Technology, Pasadena, California 91125

D. E. Jaffe, G. Masek, H. P. Paar, E. M. Potter, S. Prell, and V. Sharma
University of California, San Diego, La Jolla, California 92093

D. M. Asner, J. Gronberg, T. S. Hill, D. J. Lange, R. J. Morrison, H. N. Nelson, T. K. Nelson, and D. Roberts
University of California, Santa Barbara, California 93106

B. H. Behrens, W. T. Ford, A. Gritsan, H. Krieg, J. Roy, and J. G. Smith
University of Colorado, Boulder, Colorado 80309-0390

J. P. Alexander, R. Baker, C. Bebek, B. E. Berger, K. Berkelman, V. Boisvert, D. G. Cassel, D. S. Crowcroft, M. Dickson, S. von Dombrowski, P. S. Drell, K. M. Ecklund, R. Ehrlich, A. D. Foland, P. Gaidarev, R. S. Galik, L. Gibbons, B. Gittelman, S. W. Gray, D. L. Hartill, B. K. Heltsley, P. I. Hopman, J. Kandaswamy, D. L. Kreinick, T. Lee, Y. Liu, N. B. Mistry, C. R. Ng, E. Nordberg, M. Ogg,† J. R. Patterson, D. Peterson, D. Riley, A. Soffer, B. Valant-Spaight, A. Warburton, and C. Ward
Cornell University, Ithaca, New York 14853

M. Athanas, P. Avery, C. D. Jones, M. Lohner, C. Prescott, A. I. Rubiera, J. Yelton, and J. Zheng
University of Florida, Gainesville, Florida 32611

G. Brandenburg, R. A. Briere, A. Ershov, Y. S. Gao, D. Y.-J. Kim, R. Wilson, and H. Yamamoto
Harvard University, Cambridge, Massachusetts 02138

T. E. Browder, Y. Li, J. L. Rodriguez, and S. K. Sahu
University of Hawaii at Manoa, Honolulu, Hawaii 96822

T. Bergfeld, B. I. Eisenstein, J. Ernst, G. E. Gladding, G. D. Gollin, R. M. Hans, E. Johnson, I. Karliner, M. A. Marsh, M. Palmer, M. Selen, and J. J. Thaler
University of Illinois, Urbana-Champaign, Illinois 61801

K. W. Edwards
Carleton University, Ottawa, Ontario, Canada K1S 5B6
and the Institute of Particle Physics, Canada

A. Bellerive, R. Janicek, and P. M. Patel
McGill University, Montréal, Québec, Canada H3A 2T8
and the Institute of Particle Physics, Canada

A. J. Sadoff
Ithaca College, Ithaca, New York 14850

R. Ammar, P. Baringer, A. Bean, D. Besson, D. Coppage, C. Darling, R. Davis, S. Kotov, I. Kravchenko, N. Kwak, and L. Zhou
University of Kansas, Lawrence, Kansas 66045

S. Anderson, Y. Kubota, S. J. Lee, R. Mahapatra, J. J. O'Neill, R. Poling, T. Riehle, and A. Smith
University of Minnesota, Minneapolis, Minnesota 55455

M. S. Alam, S. B. Athar, Z. Ling, A. H. Mahmood, S. Timm, and F. Wappler
State University of New York at Albany, Albany, New York 12222

A. Anastassov, J. E. Duboscq, K. K. Gan, T. Hart, K. Honscheid, H. Kagan, R. Kass, J. Lee, H. Schwarthoff, A. Wolf, and M. M. Zoeller
Ohio State University, Columbus, Ohio 43210

S. J. Richichi, H. Severini, P. Skubic, and A. Undrus
University of Oklahoma, Norman, Oklahoma 73019

M. Bishai, S. Chen, J. Fast, J. W. Hinson, N. Menon, D. H. Miller, E. I. Shibata, and I. P. J. Shipsey
Purdue University, West Lafayette, Indiana 47907

(CLEO Collaboration)
(Received 10 August 1998; published 22 January 1999)

Using a 4.19 fb^{-1} data sample collected with the CLEO II detector at the Cornell Electron Storage Ring, we have searched for dipion transitions between pairs of Υ resonances at center of mass energies $E_{\mathrm{c.m.}}=10.58\,\mathrm{GeV}$ and $E_{\mathrm{c.m.}}=10.52\mathrm{GeV}$. We obtain the 90% confidence level upper limits $\mathcal{B}(\Upsilon(4S)\to\Upsilon(2S)\pi^+\pi^-)<3.9\times10^{-4}$ and $\mathcal{B}(\Upsilon(4S)\to\Upsilon(1S)\pi^+\pi^-)<1.2\times10^{-4}$. We also observe the transitions $\Upsilon(3S)\to\Upsilon(1S)\pi^+\pi^-$, $\Upsilon(3S)\to\Upsilon(2S)\pi^+\pi^-$, and $\Upsilon(2S)\to\Upsilon(1S)\pi^+\pi^-$, from which we measure the cross sections for the radiative processes $e^+e^-\to\Upsilon(3S)\gamma$ and $e^+e^-\to\Upsilon(2S)\gamma$. We obtain $\sigma_{ee\to\Upsilon(3S)\gamma}=(17.8\pm3.0\pm1.7)$ pb and $\sigma_{ee\to\Upsilon(2S)\gamma}=(15.5\pm1.3\pm1.4)$ pb at $E_{\mathrm{c.m.}}=10.58\,\mathrm{GeV}$, and $\sigma_{ee\to\Upsilon(3S)\gamma}=(27.3\pm5.0\pm2.6)$ pb and $\sigma_{ee\to\Upsilon(2S)\gamma}=(16.3\pm1.8\pm1.5)$ pb at $E_{\mathrm{c.m.}}=10.52\,\mathrm{GeV}$, which we compare with theoretical predictions. [S0556-2821(99)02303-6]

PACS number(s): 13.25.Gv, 13.65.+i

I. INTRODUCTION

Bottomonium dipion transitions have been the subject of many studies [1–3]. So far, theoretical efforts have concentrated on investigating dipion transitions between pairs of Υ resonances below $B\bar{B}$ threshold production, in part because of complexities in the theoretical analysis of coupled-channel effects above the $B\bar{B}$ threshold. There are no experimental results on $\Upsilon(4S)$ dipion transitions; one would generally expect very small branching fractions for such $\Upsilon(4S)$ decays due to the large Okubo-Zweig-Iizuka- (OZI-)allowed width for $\Upsilon(4S)\to B\bar{B}$. Nevertheless the large amount of CLEO II $\Upsilon(4S)$ resonance data and our familiarity with the systematics of such transitions [4] make it worthwhile to perform a dedicated search for the transitions $\Upsilon(4S)\to\Upsilon(2S)\pi^+\pi^-$ and $\Upsilon(4S)\to\Upsilon(1S)\pi^+\pi^-$.

We can also measure the cross sections for the processes $e^+e^-\to\Upsilon(3S)\gamma$ and $e^+e^-\to\Upsilon(2S)\gamma$ by reconstructing the decay chains $\Upsilon(nS)\to\Upsilon(mS)\pi^+\pi^-$, $\Upsilon(mS)\to e^+e^-,\mu^+\mu^-$ with $(n,m)=(3,1)$, (2,1), (3,2). These processes are important in determining the accuracy of theoretical calculations [5] and experimental measurements [6] of the cross section for hadron production in e^+e^- annihilations at $\sqrt{s}\approx10\,\mathrm{GeV}$. The process $e^+e^-\to\Upsilon(nS)\gamma\to\gamma+\mathrm{hadrons}$ comprises one of the largest systematic uncertainties to the measurement of $R=\sigma(e^+e^-\to\mathrm{hadrons})/\sigma(e^+e^-\to\mu^+\mu^-)$ in the Υ region.

*Permanent address: Yonsei University, Seoul 120-749, Korea.
†Permanent address: University of Texas, Austin TX 78712.

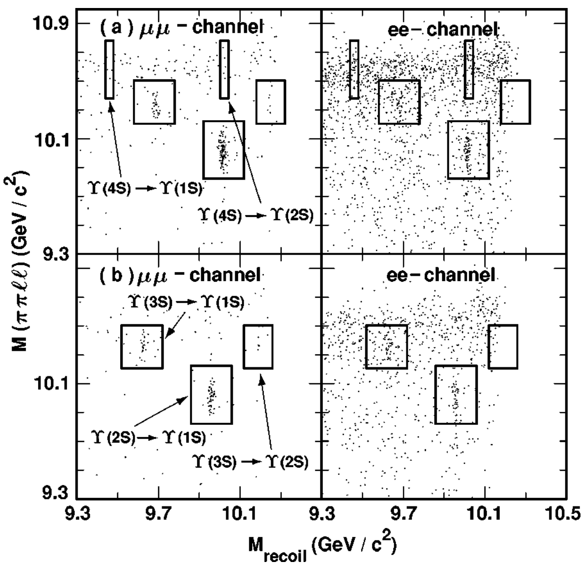

FIG. 1. Plots of $\pi\pi ll$ invariant mass vs recoil mass for the $\Upsilon(nS)\to\Upsilon(mS)\pi^+\pi^-$ transitions from data: (a) at $E_{\mathrm{c.m.}}=10.58\,\mathrm{GeV}$ [on the $\Upsilon(4S)$], (b) at $E_{\mathrm{c.m.}}=10.52\,\mathrm{GeV}$ [below the $\Upsilon(4S)$].

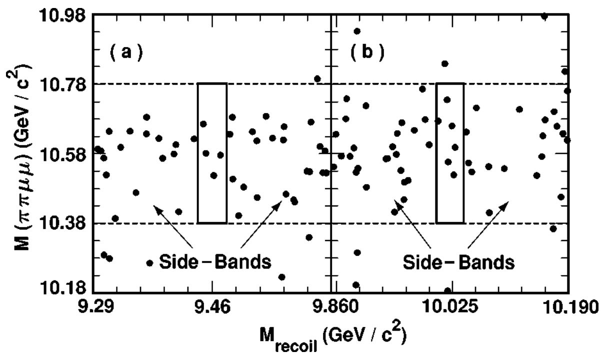

FIG. 2. The $\pi\pi\mu\mu$ invariant mass vs $\pi^+\pi^-$ recoil mass for (a) $\Upsilon(4S)\to\Upsilon(1S)\pi^+\pi^-$ and (b) $\Upsilon(4S)\to\Upsilon(2S)\pi^+\pi^-$ at $E_{\mathrm{c.m.}}=10.58\,\mathrm{GeV}$.

II. DETECTOR

The CLEO II detector, described in detail elsewhere [7], is a general-purpose magnetic spectrometer and calorimeter for measuring charged and neutral particles. The major subsystems of the detector (in order of increasing radius from the beam pipe) are the central detector, time-of-flight scintillators, the crystal calorimeter, 1.5-T superconducting coil, and the muon chambers. The central detector consists of three concentric drift chambers and is used for reconstruction of charged particle momenta and measurements of specific ionization energy loss (dE/dx) for particle identification. This system achieves a momentum resolution $(\delta p/p)^2=(0.0015p)^2+(0.005)^2$, where p is the momentum in GeV/c, and covers 95% of the solid angle. The dE/dx measurement has resolution of 6.2% for Bhabha tracks, and 7.1% for minimum ionizing hadrons. The time-of-flight system is used in two ways: for the lower-level trigger, and for measuring the flight time of particles to help in particle identification. The crystal calorimeter, which measures the energies deposited by neutral and charged particles, consists of 7800 thallium-doped cesium iodide (CsI) crystals arranged in a barrel and two endcaps. The central barrel region of the calorimeter covers 75% of the solid angle and achieves an energy resolution $\delta E/E(\%)=0.35/E^{0.75}+1.9-0.1E$, where E is the shower energy in GeV. The endcaps extend the solid angle coverage to about 95% of 4π, although they provide poorer energy resolution than the barrel region. The muon identification system, also arranged as an octagonal barrel and two endcaps, uses proportional tracking chambers for muon detection. These chambers are sandwiched between and behind the iron slabs that provide the magnetic field flux return.

In our analysis the JETSET 7.4 [8] program is used as a Monte Carlo event generator.[1] We use a GEANT3 [9] based detector simulation package to propagate and decay the final state particles in the CLEO II detector.

III. EVENT SELECTION

In our analysis of $\Upsilon(nS)\to\Upsilon(mS)\pi^+\pi^-$ transitions[2] we reconstruct the $\Upsilon(mS)$ exclusively from the decays $\Upsilon(mS)\to e^+e^-,\mu^+\mu^-$. The following selection criteria are common to all five transitions: (1) we require a total of four good quality primary charged tracks in the event with zero net charge; (2) two of them (the lepton candidates) must have momenta greater than 3.5 GeV/c and originate from the interaction region, defined as a cylindrical volume of 3 mm radius and 10 cm length aligned along the beam axis and centered on the e^+e^- collision point; (3) the other two tracks (the pion candidates) must have momenta less than 1 GeV/c and originate from a similar cylindrical volume $4\,\mathrm{mm}\times12\,\mathrm{cm}$ centered on the interaction point; (4) we identify electrons by requiring the ratio of the associated electromagnetic shower energy deposited in the calorimeter to the momentum of the matching track to be close to unity and the lateral pattern of energy deposition to be consistent with the electron hypothesis; (5) muons are identified by requiring the maximum penetration depth of the muon track candidate into the muon system absorber to be greater than three hadronic absorption lengths; (6) we require the cosine of the opening angle between the pion tracks to satisfy $\cos(p_\pi p_\pi)<0.9$ to suppress background from $e^+e^-\to e^+e^-\gamma$ events with γ-conversion when the resulting e^+e^- pair fakes a $\pi^+\pi^-$ pair; and (7) to further reduce background from $e^+e^-\to e^+e^-\gamma\to e^+e^-e^+e^-$ events we require (only in the ee channel) that at least one of the pion candidates must have its specific ionization energy loss measurement (dE/dx) within

[1] JETSET program is capable of simulating the tails of the Υ radiative production.

[2] $(n,m)=(4,1),\ (4,2),\ (3,1),\ (2,1),\ (3,2)$.

TABLE I. Efficiencies, numbers of events, branching fractions and rates for the charged $\Upsilon(4S)$ dipion transitions observed in the $\mu\mu$ channel.

Transition	ϵ (%)	$N^{observed}$	$N^{background}_{expected}$	$N^{signal}_{upper\ limit}$	$\mathcal{B}(\times 10^{-4})$	Γ (keV)
$\Upsilon(4S)\to\Upsilon(1S)$	48.6 ± 1.6	4	5.2	4.3	<1.2	<2.5
$\Upsilon(4S)\to\Upsilon(2S)$	38.3 ± 1.3	6	5.9	5.6	<3.9	<8.2

2.5 standard deviations of the value expected for pions.[3] We make no requirement on the dilepton invariant mass, because it has very small effect on the signal to background ratio while reducing the signal yields.

We search for a signal from the transitions of interest by plotting the invariant mass of the $\pi^+\pi^-l^+l^-$ system vs the mass recoiling against the dipion system $M_{recoil} = \sqrt{(E_{\mathrm{c.m.}}-\Sigma E_\pi)^2-(\Sigma \mathbf{p}_\pi)^2}$ as shown in Fig. 1: the upper plots are for $E_{\mathrm{c.m.}}=10.58$ GeV and the lower plots are for $E_{\mathrm{c.m.}}=10.52$ GeV (the boxes denote our signal regions[4]). Peaks from the $\Upsilon(3S)\to\Upsilon(1S)$ and $\Upsilon(2S)\to\Upsilon(1S)$ transitions are clearly seen in all four distributions. One can also notice a much smaller signal from the $\Upsilon(3S)\to\Upsilon(2S)$ transition in the $\mu\mu$ channel. This signal is not seen in the ee channel because of a cutoff in M_{recoil} due to the absence of dE/dx information for tracks with momentum less than ~ 100 MeV/c; such tracks do not reach into the outer drift chamber where the dE/dx measurement is performed. The shifts of the recoil mass peaks from the mass values of the $\Upsilon(1S)$ and $\Upsilon(2S)$ are due to the presence of an unobserved initial state radiation photon in the event.

IV. SEARCH FOR THE TRANSITIONS $\Upsilon(4S)\to\Upsilon(2S)\pi^+\pi^-$ AND $\Upsilon(4S)\to\Upsilon(1S)\pi^+\pi^-$

A. Extraction of upper limits

As one can see from Fig. 1, although there are data points in the signal regions for $\Upsilon(4S)\to\Upsilon(2S)\pi^+\pi^-$ and $\Upsilon(4S)\to\Upsilon(1S)\pi^+\pi^-$, there is no apparent clustering of the signal. Because of the overwhelmingly large backgrounds in the ee channel, we limit our analysis of these two transitions to the $\mu\mu$ channel. In Fig. 2 closeups of the signal regions for the $\Upsilon(4S)$ dipion transitions are shown. We employ a ''grand sideband'' technique to evaluate the background: we count the events in the sidebands[5] and extrapolate the background event yield into the signal region. Numbers of observed events and numbers of expected background events are reported in Table I, along with upper limits (at 90% confidence level) on the number of signal events. Also shown are the efficiencies calculated from Monte Carlo simulation. As a cross check we performed the scaled continuum subtraction to estimate the background, which yields consistent results, given the limited continuum statistics.

We calculate upper limits on the branching fractions and partial widths for $\Upsilon(4S)\to\Upsilon(mS)\pi^+\pi^-$ using the formula $\mathcal{B}=N^{signal}_{upper\ limit}/(\epsilon\mathcal{B}_{\mu\mu}\sigma\mathcal{L})$, where $\mathcal{B}_{\mu\mu}$ is the $\Upsilon(mS)$ muonic branching fraction taken from [10] [$\mathcal{B}_{\mu\mu}=(2.48\pm0.07)\%$ for $\Upsilon(1S)$ and $\mathcal{B}_{\mu\mu}=(1.31\pm0.21)\%$ for $\Upsilon(2S)$], $\sigma=(1.074\pm0.020)$ nb is the average measured $\Upsilon(4S)$ production cross section at the Cornell Electron Storage Ring (CESR), and $\mathcal{L}=(2.74\pm0.02)$ fb^{-1} is the integrated luminosity of our on-resonance data sample. Upper limits resulting from these calculations are[6]

$$\mathcal{B}(\Upsilon(4S)\to\Upsilon(1S)\pi^+\pi^-)<1.2\times10^{-4}\ \ (\mathrm{C.L.}=90\%),$$

$$\mathcal{B}(\Upsilon(4S)\to\Upsilon(2S)\pi^+\pi^-)<3.9\times10^{-4}\ \ (\mathrm{C.L.}=90\%).$$

B. Systematic errors

The dominant systematic errors in our search for the $\Upsilon(4S)$ dipion transitions are due to uncertainties in the $\Upsilon(1S)$ and $\Upsilon(2S)$ muonic branching fractions and in the track-finding efficiency. Other large sources of systematic errors include trigger efficiency uncertainties and the uncertainty in the $\Upsilon(4S)$ production cross section. The complete breakdown of systematic errors is given in Table II (relative errors in percent).

C. Discussion and conclusions

There are several predictions for the rates of dipion transition between heavy quarkonia states [2,3] below $B\bar{B}$ threshold. Naively, we might expect some suppression for $\Upsilon(4S)$ dipion transitions compared with the corresponding $\Upsilon(3S)$ transitions because of an additional node in the $\Upsilon(4S)$ wave function; this is compensated, to some extent, by the larger available phase space in the $\Upsilon(4S)$ transition. Unfortunately, the proximity of the $\Upsilon(4S)$ resonance to the

[3]The dE/dx requirement is used only in the second part of our analysis. The dE/dx measurement allows typical e/π separation on the level of 3.5 resolutions in the case of $\Upsilon(3S)\to\Upsilon(1S)$ transition and on the level of 1.5 resolutions in the case of $\Upsilon(2S)\to\Upsilon(1S)$ transition.

[4]For the $\Upsilon(4S)$ transitions the sizes of the signal regions are defined as a box ±3 standard deviations wide in each of the variables M_{recoil} and $m_{\pi\pi ll}$. This numerically corresponds to $(9.44,9.48)\cap(10.38,10.78)$ for $\Upsilon(4S)\to\Upsilon(1S)\pi\pi$ and $(10.003,10.043)\cap(10.38,10.78)$ for $\Upsilon(4S)\to\Upsilon(2S)\pi\pi$. For all other transitions the sizes of the signal regions are somewhat arbitrary.

[5]The sidebands are the horizontal strips of dimensions $(9.29,9.63)\cap(10.38,10.78)$ for $\Upsilon(4S)\to\Upsilon(1S)\pi\pi$ and $(9.853,10.193)\cap(10.38,10.78)$ for $\Upsilon(4S)\to\Upsilon(2S)\pi\pi$ in the variables M_{recoil} and $m_{\pi\pi ll}$, respectively, excluding the signal regions.

[6]We follow the procedure described in the Particle Data Group [11], and incorporate systematic uncertainties according to [12].

TABLE II. Sources and magnitudes of systematic errors in $\Upsilon(4S)\to\Upsilon(mS)\pi\pi$ transitions.

Source	Systematic error (%)	
	$\Upsilon(4S)\to\Upsilon(1S)\pi^+\pi^-$	$\Upsilon(4S)\to\Upsilon(2S)\pi^+\pi^-$
Tracking	2.8	2.8
Finite MC sample	1.0	1.0
Trigger efficiency	1.5	1.5
$\Upsilon(4S)$ production cross section	2.0	2.0
Luminosity	0.9	0.9
Υ muonic branching ratio	2.8	16.0
Total	4.9	16.5

$B\bar{B}$ threshold leads to the necessity of estimating coupled-channel contributions to the transition rates. Although there exists a model for calculating coupled-channel effects from the virtual process $\Upsilon\to B\bar{B}\to\Upsilon'$ [3], there is no such model for the real mixing of Υ and $B\bar{B}$ states, and therefore no theoretical predictions for the $\Upsilon(4S)$ transition rates.

In Table III we list for comparison values of previously measured total and partial widths of the Υ resonances [10], and our measured upper limits on the branching fraction and partial width for the $\Upsilon(4S)\to\Upsilon(1S)\pi^+\pi^-$ transition.

V. MEASUREMENT OF THE CROSS SECTIONS $e^+e^-\to\Upsilon(3S)\gamma$ AND $e^+e^-\to\Upsilon(2S)\gamma$

A. Extraction of cross sections

The same set of selection criteria used in our study of $\Upsilon(4S)$ dipion transitions was used in reconstruction of $\Upsilon(nS)$ radiative production events $e^+e^-\to\Upsilon(nS)\gamma$, $\Upsilon(nS)\to\Upsilon(mS)\pi^+\pi^-$, $\Upsilon(mS)\to e^+e^-,\mu^+\mu^-$ (Fig. 3). Generally, we do not observe the initial state radiation photon; its presence is inferred from the shift of the observed M_{recoil} peaks from the mass values of the corresponding $\Upsilon(mS)$. This mass shift is roughly equal to E_γ, the photon energy (Table IV). Because of the narrowness of the $\Upsilon(nS)$ resonances, the photons can be considered monochromatic. Effects due to the long Breit-Wigner tails of the Υ resonances are also included in our Monte Carlo efficiencies.

We obtain the number of signal $\Upsilon(nS)$ radiative production events by fitting the recoil mass distributions corresponding to the data points inside our signal regions in Fig. 1. In Fig. 4 the M_{recoil} distributions from data taken at $E_{\text{c.m.}}=10.58$ GeV are shown; the same distributions from the data taken at $E_{\text{c.m.}}=10.52$ GeV are shown in Fig. 5. We see clear signals in the $\mu\mu$ channel for all three transitions of interest. In the ee channel only the transition $\Upsilon(2S)\to\Upsilon(1S)\pi^+\pi^-$ has a clear peak while the transition $\Upsilon(3S)\to\Upsilon(1S)\pi^+\pi^-$ shows high background and the transition $\Upsilon(3S)\to\Upsilon(2S)\pi^+\pi^-$ is not seen at all because of the M_{recoil} cutoff mentioned earlier. As a fitting function we use a Gaussian for the signal, plus a linear function to represent the background. In all cases the Gaussian width is fixed at the value from the corresponding fit of the Monte Carlo signal. As a check, we have also allowed the Gaussian widths to float in the $\mu\mu$ channel and used those widths to fit the ee channel, obtaining consistent results.

In Tables V and VI we report the efficiencies (obtained from a Monte Carlo simulation), yields, confidence levels of fits, and calculated cross sections for the processes $e^+e^-\to\Upsilon(nS)\gamma$, using the formula $\sigma=N^{yield}/\epsilon\mathcal{L}B_{\pi\pi}\mathcal{B}_{ll}$. The numbers in Table V are for $E_{\text{c.m.}}=10.58$ GeV data, and those in Table VI are for $E_{\text{c.m.}}=10.52$ GeV data. Relevant branching fractions are taken from the Particle Data Group [10]. The luminosity is $\mathcal{L}=2.74\ \text{fb}^{-1}$ for our $E_{\text{c.m.}}=10.58$ GeV data sample and $\mathcal{L}=1.45\ \text{fb}^{-1}$ for our $E_{\text{c.m.}}=10.52$ GeV data sample. Appropriately combining the results from both dilepton channels we obtain the following averages for the cross sections for $e^+e^-\to\Upsilon(nS)\gamma$ [we do not include $\Upsilon(3S)\to\Upsilon(2S)\pi\pi$ data in the averages]:

at $E_{\text{c.m.}}=10.58$ GeV:

$$\sigma(e^+e^-\to\Upsilon(3S)\gamma)=17.8\pm3.0\pm1.7\ \text{pb},$$

$$\sigma(e^+e^-\to\Upsilon(2S)\gamma)=15.5\pm1.3\pm1.4\ \text{pb},$$

at $E_{\text{c.m.}}=10.52$ GeV:

TABLE III. Total and partial widths of the Υ resonances (the subscript $\pi\pi$ refers to transitions $\Upsilon(nS)\to\Upsilon(1S)\pi^+\pi^-$); all numbers, except $B_{\pi\pi}$ and $\Gamma_{\pi\pi}$ for the $\Upsilon(4S)$, are from [10].

Resonance	Γ_{total} (keV)	B_{ee} (%)	Γ_{ee} (keV)	$B_{\pi\pi}$ (%)	$\Gamma_{\pi\pi}$ (keV)
$\Upsilon(1S)$	52.5 ± 1.8	2.52 ± 0.17	1.32 ± 0.05		
$\Upsilon(2S)$	44 ± 7	1.18 ± 0.20	0.52 ± 0.03	18.5 ± 0.8	8.14 ± 1.34
$\Upsilon(3S)$	26.3 ± 3.5	1.81 ± 0.17[a]	0.48 ± 0.08	2.8 ± 0.6	0.74 ± 0.19
$\Upsilon(4S)$	$(10\pm4)\times10^3$	$(2.8\pm0.7)\times10^{-3}$	0.25 ± 0.03	<0.012	<1.2

[a]Assuming $e\mu$ universality.

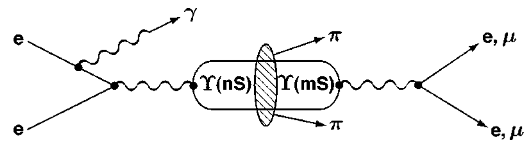

FIG. 3. Diagram for radiative production of the Υ resonances with subsequent dipion transitions.

$$\sigma(e^+e^-\to\Upsilon(3S)\gamma)=27.3\pm5.0\pm2.6\,\text{pb},$$

$$\sigma(e^+e^-\to\Upsilon(2S)\gamma)=16.3\pm1.8\pm1.5\,\text{pb}.$$

B. Systematic errors

The sources and magnitudes of systematic errors are very similar to those in our $\Upsilon(4S)$ dipion transitions measurement. Two large additional errors are the uncertainties in the dipion branching ratios and the uncertainties in the shape of the fitting function. To estimate the uncertainties in the fitting function shape, we determine how much the signal yields change when we vary the functions representing the signal and the background: we used a single Gaussian and the Monte Carlo signal shape as the signal function, and different order polynomials and Chebyshev polynomials as the background function, in various combinations. In the ee channel there is another systematic error due to uncertainties in the dE/dx measurement. We estimate this error by looking at fluctuations of our extracted values of the cross sections when we vary the dE/dx requirement. A summary of our systematic errors is given in Table VII.

C. Discussion and conclusions

Knowledge of the cross sections for the radiative processes $e^+e^-\to\Upsilon\gamma$ can increase the accuracy of the measurement of $R=\sigma(e^+e^-\to\text{hadrons})/\sigma(e^+e^-\to\mu^+\mu^-)$ at $\sqrt{s}\approx10$ GeV. Better knowledge of R allows for better determination of α_s in this low-energy region, therefore for a better test of the evolution of α_s as predicted by QCD.

Chetyrkin, Kühn, and Teubner (CKT) [5] performed a thorough calculation of the contributions to the total hadronic cross section at $E_{\text{c.m.}}=10.52$ GeV from the radiative production of the Υ resonances (Fig. 6). In Table VIII we compare our measurements of the $\Upsilon(nS)$ radiative production cross sections with their predictions. Because we extract the total $e^+e^-\to\Upsilon(nS)\gamma,\Upsilon(nS)\to$anything cross sections from our results (not just the hadronic part $e^+e^-\to\Upsilon(nS)\gamma,\Upsilon(nS)\to$hadrons, as is done in [5]), numbers for the predicted cross sections in Table VIII are scaled up by factors of 1.057, 1.041, and 1.081 for $\Upsilon(3S)$, $\Upsilon(2S)$, and $\Upsilon(1S)$, respectively, to account for the Υ leptonic decays.

TABLE IV. The initial state radiation photon energies and the recoil mass peak positions for $E_{\text{c.m.}}=10.58(10.52)$ GeV.

Transition	E_γ (GeV)	M_{recoil}^{peak} (GeV)
$\Upsilon(3S)\to\Upsilon(1S)$	0.23(0.17)	9.67(9.61)
$\Upsilon(2S)\to\Upsilon(1S)$	0.56(0.50)	10.02(9.96)
$\Upsilon(3S)\to\Upsilon(2S)$	0.23(0.17)	10.25(10.19)

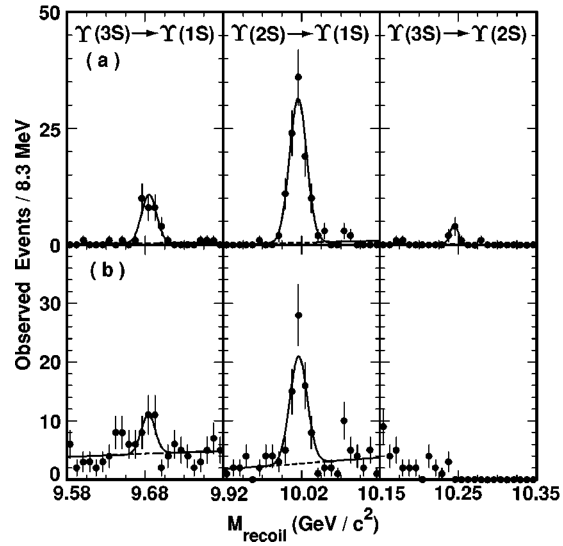

FIG. 4. Fits to the recoil mass distributions for the transitions $\Upsilon(nS)\to\Upsilon(mS)\pi^+\pi^-$ at $E_{\text{c.m.}}=10.58$ GeV for (a) $\mu\mu$ channel and (b) ee channel.

We note that similar ratios for the $\Upsilon(nS)$ radiative production cross sections can be obtained from the following simple-minded arguments: (1) the initial state radiation photon spectrum varies as $dN/dE_\gamma\sim1/E_\gamma$, and (2) the production of Υ resonances is proportional to their dielectron widths Γ_{ee}. Then one would expect for the production cross section

$$\sigma(e^+e^-\to\Upsilon\gamma)\propto\frac{\Gamma_{ee}}{E_\gamma}.$$

At $E_{\text{c.m.}}=10.58$ GeV this formula gives the ratio 2.3:1.0:1.3 for the radiative production cross sections $\sigma^{\Upsilon(3S)}:\sigma^{\Upsilon(2S)}:\sigma^{\Upsilon(1S)}$, which is very close to the CKT predictions.

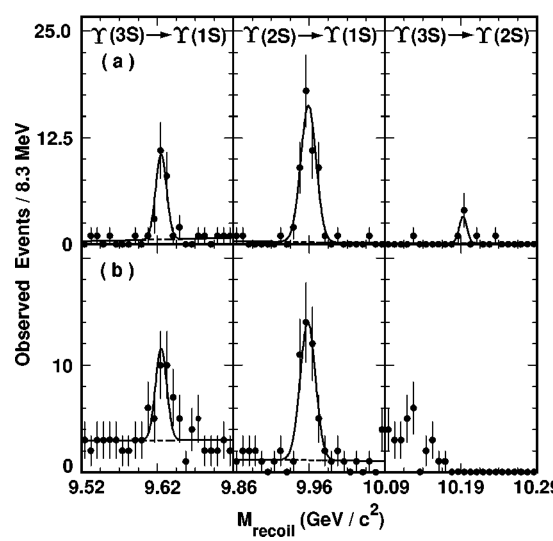

FIG. 5. Fits to the recoil mass distributions for the transitions $\Upsilon(nS)\to\Upsilon(mS)\pi^+\pi^-$ at $E_{\text{c.m.}}=10.52$ GeV for (a) $\mu\mu$ channel and (b) ee channel.

TABLE V. Efficiencies, yields, C.L. of fit, and cross sections for $e^+e^- \to \Upsilon(nS)\gamma$ at $E_{\mathrm{c.m.}} = 10.58$ GeV.

Transition	Channel	ϵ (%)	N^{yield}	C.L. (%)	σ (pb)
$\Upsilon(3S)\to\Upsilon(1S)$	$\mu\mu$	50.6±2.0	29.8±5.7	75.8	19.3±3.7±1.8
	ee	40.1±1.6	18.1±6.3	58.5	15.2±5.1±1.8
$\Upsilon(2S)\to\Upsilon(1S)$	$\mu\mu$	46.9±1.8	102.1±10.4	17.1	17.3±1.8±1.5
	ee	35.7±1.5	61.1±8.9	3.0	13.4±2.0±1.5
$\Upsilon(3S)\to\Upsilon(2S)$	$\mu\mu$	14.8±1.4	6.5±2.7	78.6	43.7±17.8±12.3
	ee	8.6±0.9			

TABLE VI. Efficiencies, yields, C.L. of fit, and cross sections for $e^+e^- \to \Upsilon(nS)\gamma$ at $E_{\mathrm{c.m.}} = 10.52$ GeV.

Transition	Channel	ϵ (%)	N^{yield}	C.L. (%)	σ (pb)
$\Upsilon(3S)\to\Upsilon(1S)$	$\mu\mu$	49.6±1.9	21.5±4.9	89.5	26.8± 6.1±2.6
	ee	41.4±1.7	19.2±5.9	91.6	28.2± 8.6±3.3
$\Upsilon(2S)\to\Upsilon(1S)$	$\mu\mu$	43.7±1.7	48.6±7.1	70.9	16.7± 2.4±1.4
	ee	36.5±1.5	39.1±6.8	47.0	15.8± 2.8±1.8
$\Upsilon(3S)\to\Upsilon(2S)$	$\mu\mu$	15.2±1.4	4.8±2.3	46.9	58.9±27.9±16.5
	ee	9.2±0.9			

TABLE VII. Sources and magnitudes of systematic errors for $e^+e^- \to \Upsilon(nS)\gamma$.

	Systematic error (%)		
Source	$\Upsilon(3S)\to\Upsilon(1S)\pi^+\pi^-$	$\Upsilon(2S)\to\Upsilon(1S)\pi^+\pi^-$	$\Upsilon(3S)\to\Upsilon(2S)\pi^+\pi^-$
Tracking	2.8	2.8	8.5
Finite MC sample	1.0	1.0	1.0
Trigger efficiency	1.5	1.5	1.5
Luminosity	0.9	0.9	0.9
Fitting function	6.8	5.4	1.0
Leptonic branching ratios	6.7/2.8[a]	6.7/2.8[a]	16.0
Dipion branching ratios	4.7	4.3	21.0
dE/dx requirement	2.2[b]	4.1[b]	
Total	11.4/9.4	11.0/9.2	27.8

[a]Separately for $ee/\mu\mu$ channels.
[b]For ee channel only.

TABLE VIII. Experimental and theoretical[a] values for the cross sections of $e^+e^- \to \Upsilon(nS)\gamma$.

	Cross section (pb)			
	$E_{\mathrm{c.m.}} = 10.52$ GeV		$E_{\mathrm{c.m.}} = 10.58$ GeV[b]	
Process	Measured	Predicted	Measured	Predicted
$e^+e^- \to \Upsilon(3S)\gamma$	27.3±5.0±2.6	41.3	17.8±3.0±1.7	30.7
$e^+e^- \to \Upsilon(2S)\gamma$	16.3±1.8±1.5	18.0	15.5±1.3±1.4	16.1
$e^+e^- \to \Upsilon(1S)\gamma$		20.4		19.2

[a]Scaled up to include contribution from $\Upsilon(nS)$ leptonic modes.
[b]Theoretical values for this energy are from [13].

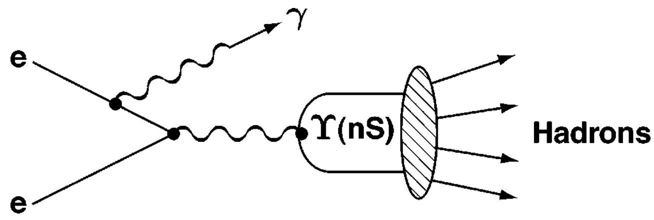

FIG. 6. Contributions from radiative production of the Υ resonances to the total hadronic cross section $e^+e^-\to$hadrons.

As seen in Table VIII, for the $\Upsilon(2S)$ case, the measured and CKT predicted values are in good agreement, while in the $\Upsilon(3S)$ case, the measured values are somewhat smaller than the predicted ones. Although the quoted systematic error in theoretical calculations is just a few permille, there may be large (on the level of 6–7 pb) shifts in the theoretical predictions due to uncertainties in the measured values of the $\Upsilon(3S)$ resonance parameters (Γ_{total},Γ_{ee}) input to the theoretical model. Such shifts could easily reconcile our results with the CKT predictions.

VI. SUMMARY

We have performed a search for the dipion transitions between Υ resonances at the center of mass energies on and below the $\Upsilon(4S)$. We set 90% confidence level upper limits on the branching fractions of the $\Upsilon(4S)$ dipion transitions: $\mathcal{B}(\Upsilon(4S)\to\Upsilon(2S)\pi^+\pi^-)<3.9\times10^{-4}$ and $\mathcal{B}(\Upsilon(4S)\to\Upsilon(1S)\pi^+\pi^-)<1.2\times10^{-4}$. By observing the transitions $\Upsilon(3S)\to\Upsilon(1S)\pi^+\pi^-$ and $\Upsilon(2S)\to\Upsilon(1S)\pi^+\pi^-$, we have measured the cross sections for the radiative processes $e^+e^-\to\Upsilon(3S)\gamma$ and $e^+e^-\to\Upsilon(2S)\gamma$. For the process $e^+e^-\to\Upsilon(2S)\gamma$ our results are in good agreement with theoretical predictions, while for the process $e^+e^-\to\Upsilon(3S)\gamma$ our measured values are somewhat below the predictions (Table VIII).

ACKNOWLEDGMENTS

We gratefully acknowledge the effort of the CESR staff in providing us with excellent luminosity and running conditions. J.R.P. and I.P.J.S. thank the NYI program of the NSF, M.S. thanks the PFF program of the NSF, M.S. and H.Y. thank the OJI program of DOE, J.R.P., K.H., M.S., and V.S. thank the A.P. Sloan Foundation, M.S. and V.S. thank the Research Corporation, S. von D. thanks the Swiss National Science Foundation, and H.S. thanks the Alexander von Humboldt Stiftung for support. This work was supported by the National Science Foundation, the U.S. Department of Energy, and the Natural Sciences and the Engineering Research Council of Canada.

[1] For a review, see M. Voloshin and Yu. Zaitsev, Usp. Fiz. Nauk **152**, 361 (1987) [Sov. Phys. Usp. **30**, 553 (1987)]; D. Besson and T. Skwarnicki, Annu. Rev. Nucl. Part. Sci. **43**, 333 (1993).
[2] T.-M. Yan, Phys. Rev. D **22**, 1652 (1980).
[3] H. Y. Zhou and Yu.-P. Kuang, Phys. Rev. D **44**, 756 (1991).
[4] CLEO Collaboration, J. P. Alexander *et al.*, Phys. Rev. D **58**, 052004 (1998).
[5] K. Chetyrkin, J. Kühn, and T. Teubner, Phys. Rev. D **56**, 3011 (1997).
[6] CLEO Collaboration, R. Ammar *et al.*, Phys. Rev. D **57**, 1350 (1998).
[7] CLEO Collaboration, Y. Kubota *et al.*, Nucl. Instrum. Methods Phys. Res. A **320**, 66 (1992).
[8] T. Sjostrand, ''PYTHIA 5.7 and JETSET 7.4: Physics and Manual,'' CERN-TH-7112-93 (1994).
[9] R. Brun *et al.*, ''GEANT3 Users Guide,'' CERN DD/EE/84-1 (1987).
[10] Particle Data Group, R. M. Barnett *et al.*, Phys. Rev. D **54**, 1 (1996), p. 547.
[11] Particle Data Group, R. M. Barnett *et al.*, Phys. Rev. D **54**, 1 (1996), p. 166; O. Helene, Nucl. Instrum. Methods **212**, 319 (1983).
[12] D. Cousins and V. Highland, Nucl. Instrum. Methods Phys. Res. A **320**, 331 (1992).
[13] T. Teubner (private communication).